

ORIGINAL ARTICLE

Open Access



Horizontal Shear Behaviors of Normal Weight and Lightweight Concrete Composite T-Beams

Zhuangcheng Fang¹, Haibo Jiang^{1*} , Airong Liu², Jiahui Feng¹ and Yuanhang Chen¹

Abstract

This paper presents the results of recent research on the interface shear behavior of normal weight and lightweight concrete composite T-beams. In the experimental program 12 beams and necessary control cylinders were tested to provide experimental cases with the variables of interface preparation, clamping stress and lightweight slab concrete strength. Compared with 7 equations developed previously, it has been found that those formulas, especially the ones from current AASHTO and ACI design codes, give a conservative theoretical prediction of horizontal shear capacity of composite T-beams. Based on the experimental results, a more accurate equation was developed to predict the interface shear transfer strength of composite concrete T-beam. By comparing the experimental results of previous beam tests and shear-friction push-off tests for different types of concrete with both rough and smooth interface published in literature, it has been found that the proposed formula is reliable in predicting the horizontal shear strength of concrete composite T-beams.

Keywords: horizontal shear behaviors, composite T-beam, lightweight concrete, normal weight concrete, interface

1 Introduction

More and more bridges now are designed and constructed with precast normal weight concrete web and cast-in-place lightweight concrete flange, such as Jiujiang Yangtze River Bridge on the G105 Highway in China, Fen-river Bridge on the G4 Highway in China, and so on. This composite construction is an economical way of combining precast and cast-in-place structure but retaining the efficiency and continuity of monolithic construction. Previous research has found that horizontal shear behavior of interface between precast web and cast-in-place flange of composite beam is crucial for development of flexural strength, diagonal shear strength, and deflection characteristics (Saemann and Washa 1964). After interface shear failure, the composite action of beams decreases, causing a significant reduction of

stiffness and flexural capacity. It has also been found that the shear behavior of interface between precast web and cast-in-place flange supported the shear-friction theory, which was first proposed by Birkeland and Birkeland (1966) and now has been adopted in ACI 318-14 (2014). Horizontal shear strength of composite concrete beams mainly depended on the interface preparation of shear surface, the ratio of shear reinforcement and the concrete strength.

In early studies, Saemann and Washa (1964) studied the strength of joint between precast concrete beams and cast-in-place concrete slabs of 42 composite concrete T-beams. It has been found complex relations exist between roughness of joint surface, ratio of reinforcement across joint and shear span.

Based on testing 16 composite concrete beams with rough interface, Loov and Patnaik (1994) proposed a parabolic equation, which took into account the effect of concrete strength and clamping stress. This proposed equation was equally applicable for both lightweight and sand-lightweight concrete.

*Correspondence: hbjiang@gdut.edu.cn

¹ School of Civil and Transportation Engineering, Guangzhou Higher Education Mega Center, Guangdong University of Technology, Guangzhou 510006, China

Full list of author information is available at the end of the article
Journal information: ISSN 1976-0485 / eISSN 2234-1315

Another insight into the interface behavior was developed by Patnaik (2001) for composite concrete beams with a smooth interface. It has been found that the current ACI design code was too conservative and a more suitable equation is needed to predict the shear transfer strength of smooth interface composite concrete beams.

To evaluate current composite beam design provisions for high-strength concrete beams, Kahn and Slapkus (2004) completed 6 composite T-beams tests with web concrete strength up to 83.6 MPa. The beams with 50.2 MPa concrete flanges all failed in horizontal shear, while the beams with the 77.8 MPa concrete flanges all failed in flexure. It suggested that both AASHTO (2015) and ACI (2014) provision for interface shear of composite beams could be applied conservatively to composite sections constructed with high-strength concrete.

Interface shear behavior had also been investigated deeply with normal weight concrete push-off tests (Mattock and Hawkins 1972; Mattock 1974; Walraven 1987; Bass et al. 1989; Harries et al. 2012) and lightweight push-off tests (Mattock et al. 1976; Shaw and Sneed 2014; Sneed et al. 2016) and several design formulas had also been proposed based on their results.

Based on composite push-off tests, Jiang et al. (2016) have found that the interface shear behavior between normal weight concrete and lightweight concrete could be explained by the shear-friction theory. However, the applicability of current shear-friction design provision was questionable for composite construction interface, because all of them were proposed based on specimens made of the same type of concrete in the web and the flange of a composite T-beam. This highlights the importance to examine the interface shear behavior between different types of concrete, especially for composite beams with normal weight concrete girder and lightweight concrete slab.

However, no relevant studies have been focused on the interface shear behavior between precast normal weight concrete web and lightweight cast-in-place concrete flange composite concrete T-beams. This study attempts to provide a useful insight of interface shear behavior between normal weight and lightweight concrete composite beams.

2 Calculation of Interface Shear Stress

When investigating the interface behavior of a composite beam, it is necessary to review the common equations for calculating the interface shear stress. More than 30 shear-friction equations have been proposed up to now, which may be divided into two categories. Those in first category are expressed as a linear equation as suggested by Mattock et al. (1976), Kahn and Mitchell (2002), ACI code (2014), AASHTO LOFD (2015), etc.; and those in second category

are expressed as a parabolic equation as suggested by Walraven (1987), Loov and Patnaik (1994). 7 equations which were commonly used and applicable for predicting the interface shear capacity are given as follows.

2.1 Mattock et al. Equation

Mattock et al. (1976) examined the direct shear transfer across an interface of lightweight concrete with the variable of aggregate type, concrete strength, shear reinforcement ratio and preparation of interface. A linear design equation for nominal shear stress v_n is recommended as follows:

$$v_n = 1.4\rho f_y + 1.72 \leq \text{the smaller of } 0.2f'_c \text{ or } 5.5 \text{ MPa} \quad (1)$$

where v_n = nominal shear stress, MPa; ρf_y = clamping stress, MPa; f'_c = concrete cylinder compressive strength, MPa.

2.2 Walraven's Equation

Walraven (1987) conducted 88 push-off tests with concrete compressive strength up to 62.06 MPa to make a statistical analysis of aggregate interlock effect. The following parabolic equation is proposed:

$$v_n = C_1 (\rho f_y)^{C_2} \quad (2)$$

where $C_1 = 0.878 f_c^{0.406}$ and $C_2 = 0.167 f_c^{0.303}$.

2.3 Loov and Patnaik's Equation

Loov and Patnaik (1994) proposed another applicable equation for both lightweight and normal weight concrete based on the experimental results of 16 composite beams. This parabolic equation is referred as follows:

$$v_n = k\lambda\sqrt{(0.1 + \rho_v f_y)f'_c} \leq 0.25f'_c \quad (3)$$

where k = roughness constant, 0.6 for rough surface and 0.5 for smooth surface; λ = correction factor related to concrete weight, 1 for normal weight concrete and 0.85 for lightweight concrete.

2.4 Kahn and Mitchell's Equation

Kahn and Mitchell (2002) performed 50 push-off tests of concrete beams made of concrete strength up to 123.4 MPa and found that the current design code underestimated the shear strength for high-strength concrete. A more accurate linear equation, which was adapted for monolithic, rough and cold-joint surface condition, is provided as follows:

$$v_n = 0.05f'_c + 1.4\rho f_y \leq 0.2f'_c \quad (4)$$

2.5 ACI Design Code

ACI 318-14 (2014) gives Eq. (5) as the general relation for a clean, rough shear interface with the upper limit of $3.45 b_v d$ in Sect. 16.4.4-Nominal horizontal shear strength:

$$v_n = (1.8 + 0.6\rho f_y)\lambda b_v d \leq 3.45 b_v d \quad (5)$$

where b_v = width of interface, m; d = effective depth of tension reinforcement, m.

Another shear-friction equation (Eq. 6) was proposed further in Sect. 22.9.4—Nominal shear strength of ACI 318-14 (2014) to use for shear stress greater than $3.45 b_v d$. This linear equation is given as follows:

$$v_n = \mu \rho f_y \leq \text{the smaller of } 0.2f'_c \text{ or } 5.5 \text{ MPa} \quad (6)$$

where $\lambda = 1$ for normal weight concrete and 0.85 for lightweight concrete; μ = coefficient of friction, 1.4 for monolithic concrete connection, 1.0 for a cold-joint surface with 6.4 mm roughness amplitude and 0.6 for a smooth cold-joint interface.

2.6 AASHTO Design Code

Compared with ACI shear-friction formula, another shear-friction equation considering the cohesion factor is recommended in Sect. 5.8.4-Interface shear transfer shear friction of AASHTO LRFD (2015) as follows:

$$V_n = cA_{cv} + \mu [A_v f_y + P_c] \leq V_{nmax} \quad (7)$$

where c = cohesion coefficient, 1.9 MPa for rough interface condition and 0.52 MPa for smooth interface condition, μ = friction factor, 1.0 for rough surface and 0.6 for smooth surface, P_c = the permanent net compressive force, kN. A_v = the area of concrete shear interface, m². An upper limitation of $0.3 f'_c$ and 9.0 MPa was proposed for rough shear interface and that of $0.2 f'_c$ and 5.5 MPa for smooth interface.

2.7 Determination of Interface Shear Stress

The ACI code (2014) recommends that design horizontal shear stress can be calculated across the shear interface by the following equation when a beam is uncracked and linearly elastic:

$$v_n = \frac{C}{bl} \quad (8)$$

where C = total compression in the flange, N; b = the width of interface, mm; l = length over which horizontal shear is to be transferred, mm. This equation provides common basis for comparison because of its widely use in previous studies. It can be used to calculate the horizontal shear stress for a composite beam.

3 Experimental Program

The experimental program included 12 composite concrete beams tested to investigate the interface shear behavior between normal weight concrete and lightweight concrete.

3.1 Variables

Three primary variables were investigated in this study, including interface preparation, lightweight slab concrete strength, and clamping stress. Interface preparation referred to rough shear interface condition or smooth shear interface condition. The target lightweight slab concrete strengths in composite beams were expected as 30, 40, and 50 MPa to investigate the influence of concrete strength. For the third variable, specimens were constructed with clamping stress of 0.00, 0.60, 1.21 and 2.41 MPa, which covered the practical range of clamping stresses. Additionally, specimen nomenclature corresponds to the test variable as shown in Table 1. Specimen

Table 1 Specimens designation and test matrix.

Specimens designation	Shear interface condition	Target lightweight slab concrete strength (MPa)	Quantities of shear reinforcement
R-30-5	Rough	30	5 ϕ 10 double-legged stirrups
R-40-0	Rough	40	0
R-40-5	Rough	40	5 ϕ 10 double-legged stirrups
R-40-9	Rough	40	9 ϕ 10 double-legged stirrups
R-40-17	Rough	40	17 ϕ 10 double-legged stirrups
R-50-5	Rough	50	5 ϕ 10 double-legged stirrups
S-30-5	Smooth	30	5 ϕ 10 double-legged stirrups
S-40-0	Smooth	40	0
S-40-5	Smooth	40	5 ϕ 10 double-legged stirrups
S-40-9	Smooth	40	9 ϕ 10 double-legged stirrups
S-40-17	Smooth	40	17 ϕ 10 double-legged stirrups
S-50-5	Smooth	50	5 ϕ 10 double-legged stirrups

designation indicates the interface condition (R = Rough shear interface with about 6.4 mm amplitude, and S = Smooth shear interface); the target cylinder compressive strength of lightweight slab concrete (30, 40, 50 = 30 MPa, 40 MPa and 50 MPa for lightweight slab concrete, respectively); the quantities of double-legged closed stirrup across the shear interface (0, 5, 9, 17 = none, 5, 9, and 17 $\phi 10$ double-legged stirrups crossing the shear plane, respectively).

3.2 Test Beams

Typical cross section and details of reinforcement arrangement in beam with 17 stirrup bars across the shear interface is shown in Fig. 1. Beams, with their slabs discontinued at 1200 mm from the mid-span, were designed to be similar to those of Loov and Patnaik (1994), Patnaik (2001) and Kahn and Slapkus (2004) to allow the development of a horizontal shear failure. Stronger resistance in flexure and diagonal shear were designed to ensure that specimens would fail in horizontal shear prior to failing in any other mode. Double-legged welded looped stirrups were used as shear reinforcement to achieve the desired level of clamping stress by adjusting the amount of steel crossing the interface. As the nominal transversal reinforcement ratio decreased from 0.698 to 0.349%, the reduction of stirrup steel across the shear plane in each case was

accomplished by cutting off half of the stirrups crossing the interface. Because the stirrups near the center of the span were not effective, reinforcement ratio ρ was calculated through dividing the area of stirrups (except for the mid-span stirrup) crossing the shear interface by the total surface area (2400 mm \times 150 mm). Shorter closed rectangular stirrups with diameter of 10 mm were added to provide enough shear resistance below the interface, especially for both end portions. All the stirrups were well anchored on both sides of the interface so they were able to reach yielding at the shear plane. Additionally, 4 10-mm-diameters top longitudinal reinforcements were used in the top of reinforcement cage to weld together the shear reinforcements, while 2 10-mm-diameters support reinforcements were used to tie together the shorter stirrups at end portion of the beam. All types of steel bars were from the same shipment. In summary, detail properties of reinforcement used in the specimens are given in Table 2.

3.3 Materials

Four different concrete mixes with water-cement ratio (w/c) ranging from 0.33 to 0.69 were used to make the testing beams, including one type of normal weight concrete for girder and three type of lightweight concrete for slab. Crushed granitic coarse aggregate, with grading of 100% passing a 25 mm sieve and less than 5% passing a

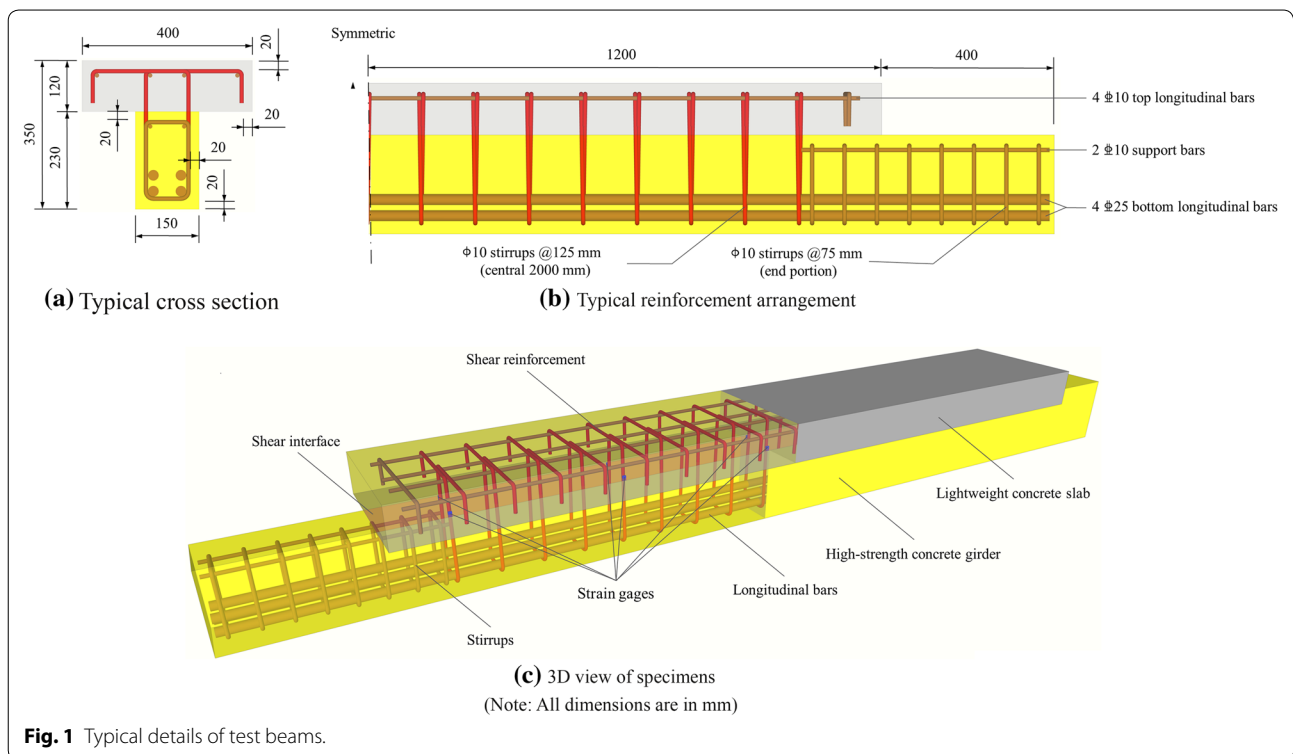


Fig. 1 Typical details of test beams.

Table 2 Detail properties of test beams.

Specimens	Concrete strength (MPa)		Stirrups crossing interface				Reinforcement ratio ρ (%)	Clamping stress ρf_y (MPa)
	Web	Flange	Spacing (mm)	Area (mm ²)	Yield strength (MPa)	Ultimate strength f_u (MPa)		
R-30-5	50.32	30.03	500	628	345.86	543.18	0.174	0.60
R-40-0	47.30	40.10	–	–	–	–	0	0
R-40-5	47.89	42.24	500	628	345.86	543.18	0.174	0.60
R-40-9	48.28	40.73	250	1256	345.86	543.18	0.349	1.21
R-40-17	51.05	40.64	125	2512	345.86	543.18	0.698	2.41
R-50-5	51.97	50.71	500	628	345.86	543.18	0.174	0.60
S-30-5	50.32	30.03	500	628	345.86	543.18	0.174	0.60
S-40-0	47.30	40.10	–	–	–	–	0	0
S-40-5	47.89	42.24	500	628	345.86	543.18	0.174	0.60
S-40-9	48.28	40.73	250	1256	345.86	543.18	0.349	1.21
S-40-17	51.05	40.64	125	2512	345.86	543.18	0.698	2.41
S-50-5	51.98	50.71	500	628	345.86	543.18	0.174	0.60

5 mm sieve, was used to make the normal weight concrete with target compressive strength of 50 MPa. A well graded lightweight expanded shale coarse aggregate with a maximum size of 20 mm was chosen for concrete mixture for slab. The same washed local river medium sand and ordinary Portland cement was used in all types of concrete. More details of concrete mixture proportions and other properties of concrete mixtures were summarized in Table 3, including density of concrete (ASTM 2017), target concrete strength f_c (ASTM 2015), concrete strength at test day f'_c (ASTM 2015), splitting tensile strength f_t (ASTM 2011); elasticity modulus E_c (ASTM 2014), and Poisson ratio μ (ASTM 2014). All the properties were determined using standard cylinders, which were cured under the conditions similar to the corresponding test beam. It can be noticed that all the beams had the same concrete strength for girder portions, which was designed to reduce the influence of web concrete as much as possible.

Properties of reinforcements are given in Table 4. Importantly, shear reinforcement crossing interface in different beams consisted of the same type of reinforcements, whose average measured yield strength was 345.86 MPa and modulus of elasticity was 1.87×10^5 MPa.

3.4 Specimens Fabrication

The casting procedure of test beams is shown in Fig. 2. The beams were constructed with plywood form to simulate composite beam with a cold-joint between precast girder and cast-in-place slab (Fig. 2a). The web portions fabricated with stirrups were cast first to mimic a

precast girder. Two types of interface had been prepared when the web concrete was still wet. The rough interface was left as-cast with some of the coarse aggregate protruding, which complied with the requirement by ACI Code (2014) as roughness amplitude of 6.4 mm. As for smooth interface, very little coarse aggregate protruded from the top surface after troweling smooth. The result surface finishes of the web are shown in Fig. 3. Webs were cured in a moist condition before casting the flange portion (Fig. 2b). All the control cylinders were cured under the same condition as those of web and flange concrete (Fig. 2d). Forms were removed at 3 days. After 14 days curing, beams were left outside the laboratory until placed in the test machine (2 months of natural curing).

3.5 Test Procedure

Beams were simply supported and loaded with a point load at central span as indicated in Fig. 4. The beams were tested with the rate of 1 mm per minute in a manual hydraulic actuator having 1000 kN capacity. Load was held constant for a while at each increment of 0.5 mm to allow marking cracks, measuring width of cracks and taking photos. A preload of 10 kN was applied to ensure that all the testing equipment was set up correctly and was then released to zero. For beams with shorten flanges, the maximum slip after failure load was always measured at the end of the flanges (Loov and Patnaik 1994). The slip near the quarter spans were also important parameters for studying shear interface behavior before the beam reached its ultimate capacity (Hanson 1960). Thus, 6 linear variable displacement transducers (LVDTs) were mounted on beams to measure the slips of the flange

Table 3 Concrete properties.

Concrete type	Mixture quantities (kg/m ³)				W/C	Density of concrete (kg/m ³)	Target f_c (MPa)	f'_c (MPa)	f_r (MPa)	E_c (MPa)	μ		
	Coarse aggregate	Fine aggregate	Water	Cement								Fly ash	Water reducer
C50 web concrete	1095	616	154	459	103	13.15	0.33	2440	50	49.47	4.09	37,389	0.20
L30 slab concrete	543	808	211	306	–	–	0.69	1868	30	30.03	3.46	26,344	0.21
L40 slab concrete	512	826	206	359	–	–	0.57	1903	40	40.93	4.20	27,949	0.19
L50 slab concrete	508	787	201	428	–	–	0.47	1924	50	50.71	4.02	31,449	0.20

Table 4 Reinforcement properties.

Type	Yield strength (MPa)	Ultimate tensile strength (MPa)	Elasticity of modulus (MPa)
Grade 40 steel bars ($\phi 10$)	345.86	543.18	1.87×10^5
Grade 40 steel bars ($\Phi 10$)	456.39	567.52	1.82×10^5
Grade 40 steel bars ($\Phi 25$)	409.12	557.31	1.79×10^5

relative to the web. Four of them were installed in pairs at both quarter spans. The other 2 LVDTs were employed in each end of the flange. They were attached with the help of a magnetic base placed on steel plates, which were firmly clamped to the top of each web at either end of the test beam. The mid-span and quarter-span vertical deflections were also recorded. To investigate the shear-friction assumption that shear reinforcement crossing the interface yielded, strain gauges were glued on selected stirrups at the location of the interface and their

strain were recorded at regular load intervals, as shown in Fig. 1c.

4 Experimental Results and Discussion

4.1 Observed Behavior

After applying a few increments of load, several flexural cracks were observed at the bottom of beams. As loading increased, more cracks formed and the initial cracks lengthened and widened. Most of the cracks propagated toward the loading point and terminated in a crack along the interface. With continuously loading, those short cracks appeared earlier along the interface joined together other and extended toward the central span. From now on, the flange slipped relative to the web away from the central span of beams. As loading further increased, the entire flange on the weaker side (that had a large slip) sheared suddenly along the interface with a large slip (more than 0.5 mm), causing a clearly visible separation and horizontal crack. Now this beam can be defined as failing in horizontal



(a) Formwork of web portions



(b) Curing of web concrete

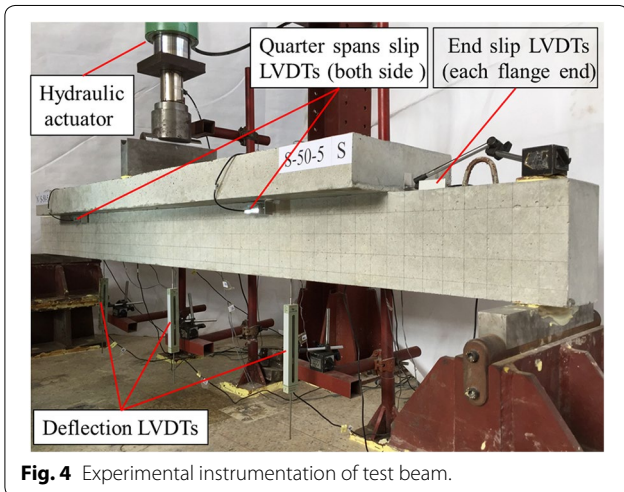


(c) Formwork of flange portions



(d) Curing of flange concrete

Fig. 2 Casting procedure of test beams.

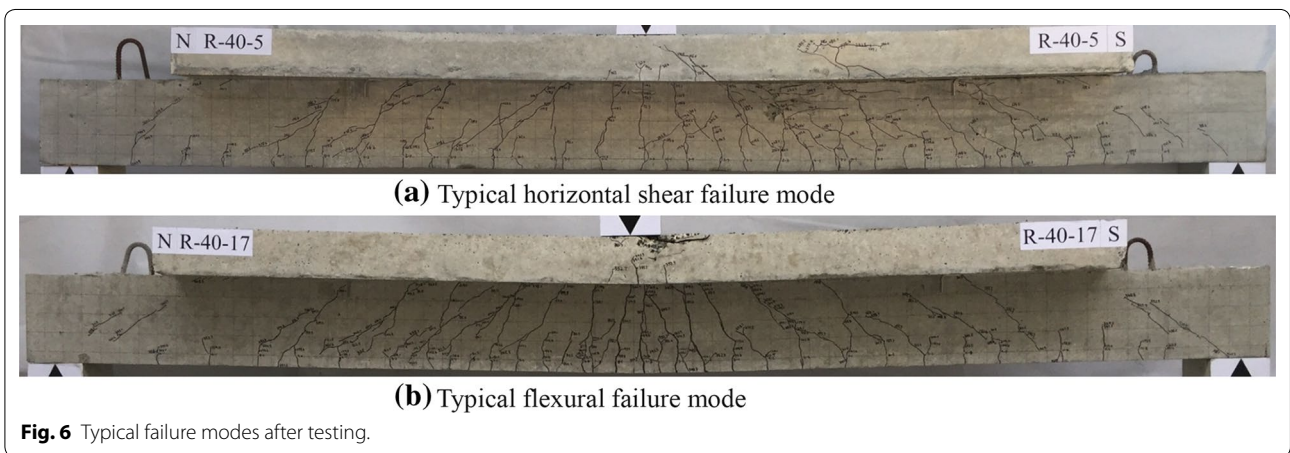
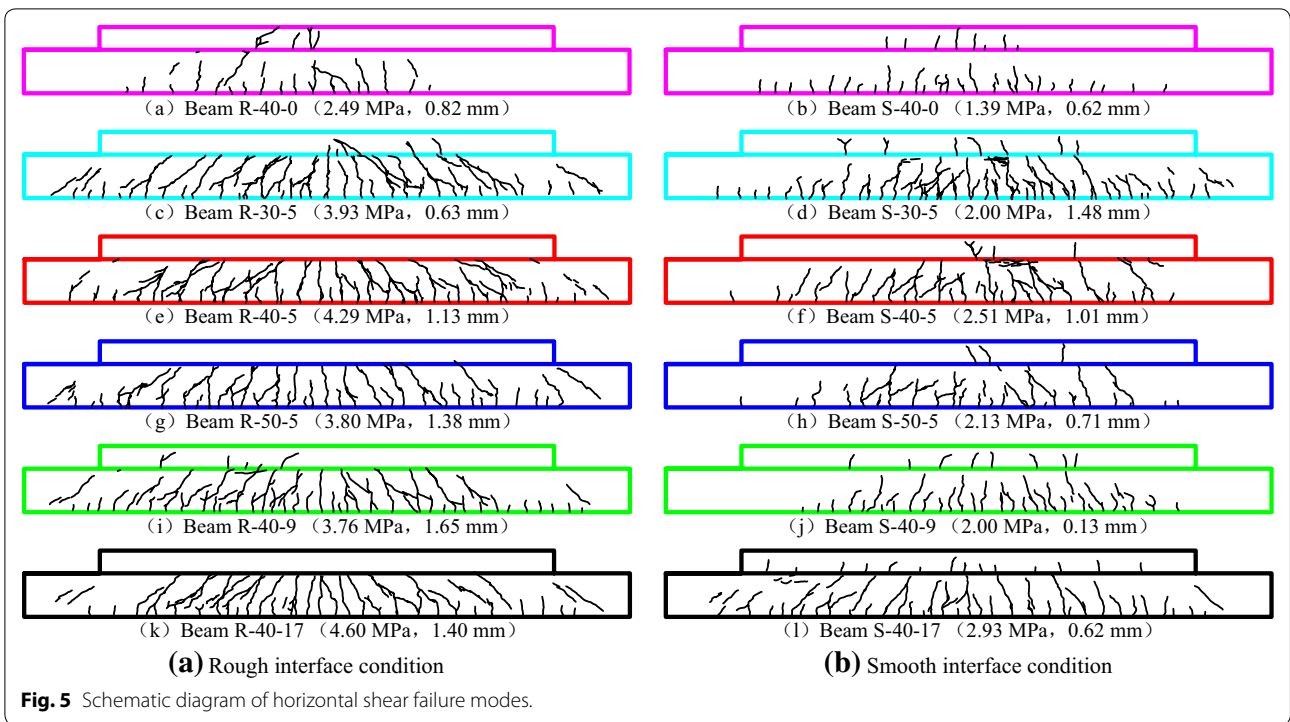


shear. This failure mode may be described as a perfect horizontal shear failure mode and was observed for all beams except for Beam R-40-17. Additionally, with increasing of loading, the final failure was usually accompanied by a compression failure in the web. Saemann and Washa (1964) had found that the beam began to act as a partially composite member and it is apparent that two-beam action exists at this time.

Figure 5 shows the horizontal shear failure mode of all beams tested in this study. All the beams failed at the interface by shear, except for Beam R-40-17. Beam R-40-17 failed in flexure with compressive crushing of the top of flange concrete appearing because of the higher interface clamping stress, and the failure mode of Beam R-40-17 corresponded to the fact that

it achieved the highest failure load among all beams tested as shown in Fig. 5. Compared with beams with rough interface, the test beams with a smooth interface have formed less flexural cracks. This may be associated with the premature failure of smooth surface, which limited the development of web bending resistance. No matter beams with rough or smooth interface condition, more flexural cracks or diagonal shear cracks were observed with the increasing of interface reinforcement ratio. More cracks appeared in beam with lower slab strength for both rough interface and smooth interface beams. From Table 3, it can be noticed that lower strength concrete has a lower elastic modulus, causing larger deflection.

Previous studies have found that the horizontal shear capacity reduced until reaching the residual stress after interface shear failure (Mattock et al. 1976; Kahn and Mitchell 2002; Shaw and Sneed 2014; Jiang et al. 2016). Figure 6 shows typical failure mode of this post-cracking behavior. Several flexure cracks appeared in the flange of these beam and lots of crush cracks formed at the top of the web below the flange. This failure mode (Fig. 6a) showed that the reduction of composite action after horizontal shear failure of composite concrete beam resulting in that the test beams acted as two beams stacked one over another. Most of the beam failed in this type of failure mode after ultimate load, except for Beam R-40-17. For Beam R-40-17, there were extensive flexural cracking in the web, but no flexural cracks appeared in the bottom of flange or crushing cracks in the top of web as shown in Fig. 6a. On the other hand, Beam R-40-17 failed in flexure where the flange concrete was crushed near the loading point (see Fig. 6b).

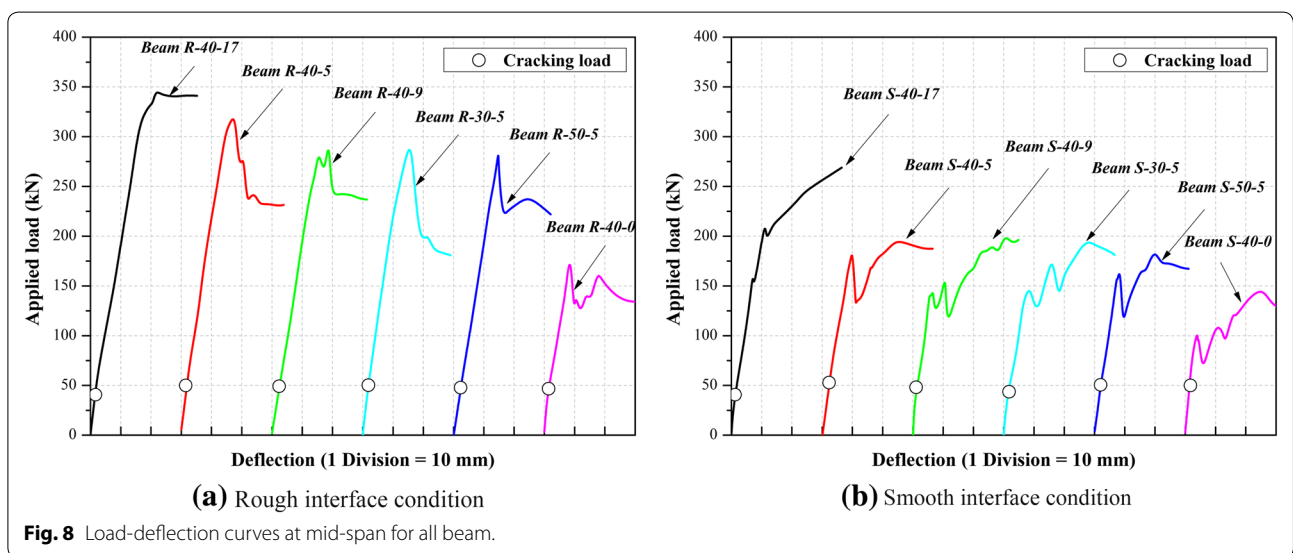
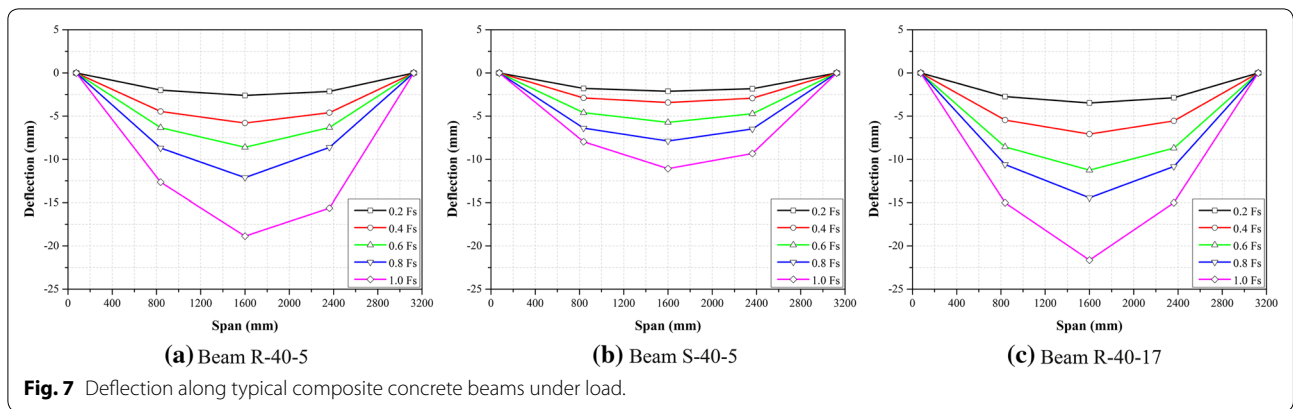


4.2 Deflection Characteristics

The vertical deflection of typical composite concrete beams at different vertical loads is plotted in Fig. 7. As the vertical load increased, the vertical deflection of composite concrete beams increased gradually, and the composite beams acted as a monolithic beam. When reaching the horizontal shear failure load F_s , as mentioned previously, the entire flange on the weaker side slipped suddenly along the interface, causing a larger quarter-span deformation at one side of the beam. It applied to all beams tested except Beam R-40-17, which

did not fail in horizontal shear rather in flexure. Obviously, the largest vertical deflection of beams occurred at mid-span.

Figure 8 shows the load–deflection curve at mid-span for all the beams. As the applied load increased, the mid-span deformation increased linearly. When the first flexural cracks appeared, this load–deflection relationship became nonlinear. This nonlinear behavior was associated with the cracking of beams, the reducing of stiffness, the material nonlinearity or even the geometric nonlinearity.



The mid-span deflection of beams at horizontal shear failure loads versus the position of beams with different interface clamping stress and different slab lightweight concrete strength is plotted in Fig. 9. It can be found that the deflection at interface shear failure load of composite beam increased with the increasing of clamping stress (except for Beam S-40-17), but independent of the lightweight concrete strength of the slab. On the other hand, the interface preparation method played an important role in mid-span vertical deformation at interface shear failure load for composite concrete beams.

4.3 Horizontal Shear Stress

Horizontal shear stress is a significant index to develop an important insight into the interface shear behavior of composite beams with different types of concrete. The interface shear stress v_n of test beam at failure loads were calculated using Eq. (8) with the cracked transformed mid-span section. Values of C in mid-span

section at shear failure, b and l for different beams are given in Table 5. It also shows the concrete compressive strength for both web and flange portions, total area of longitudinal reinforcements A_s , the depth to the neutral axis h_0 and the moment of inertia of entire cross section I . Table 6 summarizes the experimental horizontal shear stress v_n obtained from this study, the theoretical interface shear stress $v_{Eq(x)}$ predicted by the 7 methods discussed in the background section and the values of $v_n/v_{Eq(x)}$. It can be found that almost all of the equations discussed in this paper underestimated the horizontal shear stress of composite concrete beams in this study with a rough interface, except for the theoretical value calculated by Eq. (2) when predicting the horizontal shear stress for specimens with high reinforcement ratio. Compared with design code [Eqs. (5)–(7)], the equations proposed by other researchers [Eqs. (1)–(4)] gave a closer predicted results. Both the linear equation proposed by Mattock et al. (1976) [Eq. (1)] and the parabolic equation

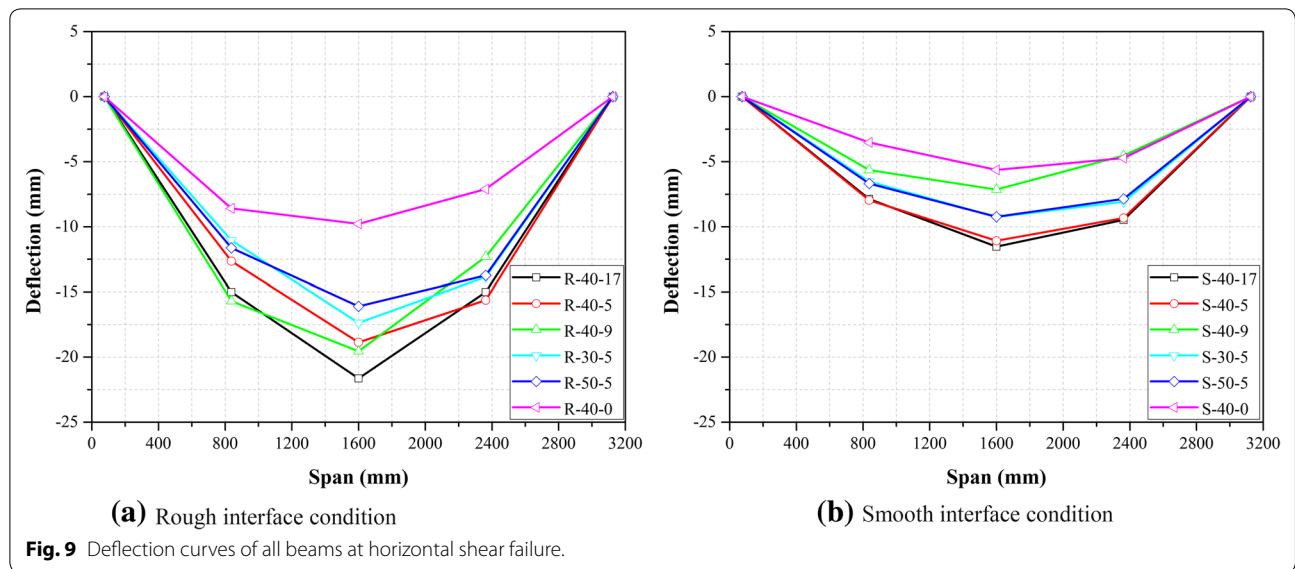


Table 5 Physical properties of test beams.

Specimens	Concrete strength f'_c (MPa)		Interface width b (mm)	Interface length l (mm)	Area of longitudinal steel A_s (mm ²)	Cracked transformed section properties		
	Web	Flange				h_0 (mm)	$I \times 10^6$ (mm ⁴)	$C \times 10^4$ (N)
R-30-5	50.32	30.03	150	1200	1964	110	610	87.0
R-40-0	47.30	40.10	150	1200	1964	107	585	54.6
R-40-5	47.89	42.24	150	1200	1964	107	585	95.0
R-40-9	48.28	40.73	150	1200	1964	107	585	87.6
R-40-17	51.05	40.64	150	1200	1964	107	585	102.1
R-50-5	51.97	50.71	150	1200	1964	102	537	84.1
S-30-5	50.32	30.03	150	1200	1964	110	610	57.7
S-40-0	47.30	40.10	150	1200	1964	107	585	44.0
S-40-5	47.89	42.24	150	1200	1964	107	585	57.5
S-40-9	48.28	40.73	150	1200	1964	107	585	59.9
S-40-17	51.05	40.64	150	1200	1964	107	585	79.3
S-50-5	51.98	50.71	150	1200	1964	102	537	54.2

suggested by Eq. (3) gave a reasonably acceptable estimation for smooth interface condition, but underestimated the strength of specimens with rough interface condition. On the contrary, Eqs. (2) and (4) were able to fit the results better for beams with rough surface but not conservative for smooth surface beams. Design code formulas, especially for ACI shear friction [Eq. (6)], provided a too conservative theoretical results for composite beam tested in this study.

4.4 Horizontal Shear Stress v_n -Slip Relations

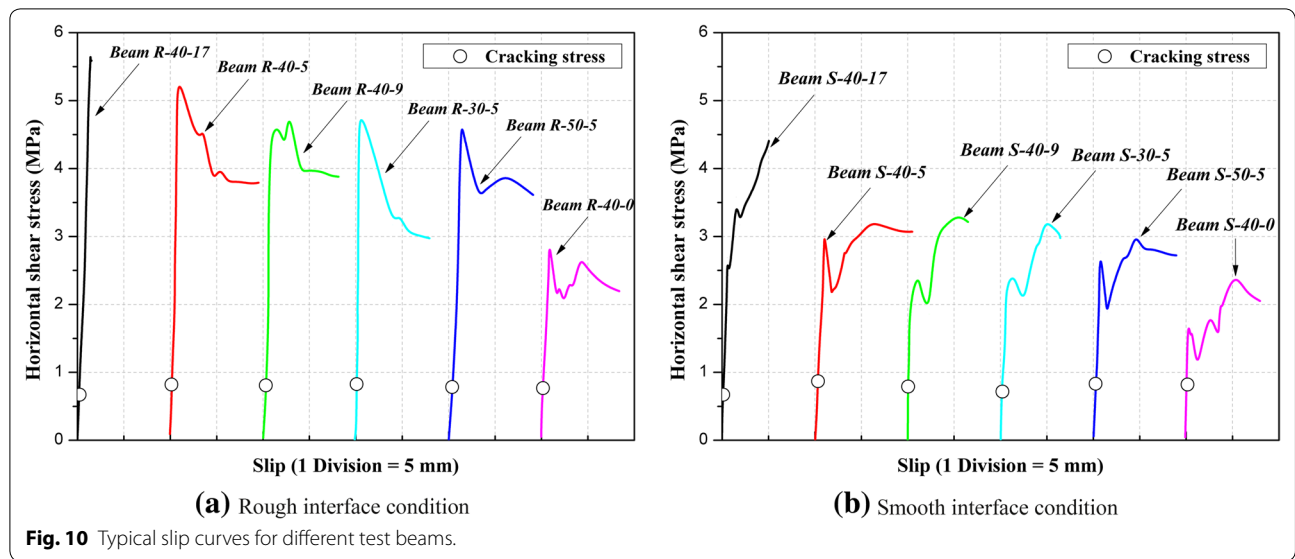
The slip of shear interface is a significant index for evaluating the composite action of beam, which is defined as

the slippage of flange relative to the web. At horizontal shear failure load, the maximum slips always occurred at the end of flange on the weaker side. In Fig. 10, horizontal shear stress v_n is plotted versus slip at the point along each beam where the maximum slip recorded. The slips which developed in beams with different interface preparation were not similar. For rough interface condition, the slip increased simultaneously at a slower rate with the increasing of horizontal shear stress. The slip then increased suddenly with a sudden drop in horizontal shear stress. It was the horizontal shear failure that occurred at the interface between lightweight concrete flange and normal weight concrete web. After interface

Table 6 Comparison of experimental results with theoretical prediction.

Specimens	Experimental v_r	Mattock et al. Eq. (1)		Walraven Eq. (2)		Loov and Patnaik Eq. (3)		Kahn and Mitchell Eq. (4)		ACI Eq. (5)		ACI shear-friction Eq. (6)		AASHTO LRFD Eq. (7)	
		$V_{Eq. (1)}$	$V_r/V_{Eq. (1)}$	$V_{Eq. (2)}$	$V_r/V_{Eq. (2)}$	$V_{Eq. (3)}$	$V_r/V_{Eq. (3)}$	$V_{Eq. (4)}$	$V_r/V_{Eq. (4)}$	$V_{Eq. (5)}$	$V_r/V_{Eq. (5)}$	$V_{Eq. (6)}$	$V_r/V_{Eq. (6)}$	$V_{Eq. (7)}$	$V_r/V_{Eq. (7)}$
R-30-5	4.83	2.20	2.19	2.76	1.75	1.95	2.48	2.34	2.06	1.83	2.64	0.51	9.44	2.50	1.93
R-40-0	3.03	1.72	1.76	0.00	0.00	0.85	3.56	2.01	1.51	1.52	1.99	0.00	0.00	1.90	1.59
R-40-5	5.28	2.20	2.40	3.08	1.71	2.31	2.28	2.95	1.79	1.83	2.89	0.51	10.32	2.50	2.11
R-40-9	4.62	2.69	1.72	4.36	1.06	3.10	1.49	3.73	1.24	2.14	2.16	1.03	4.50	3.11	1.49
R-40-17	5.67	3.65	1.55	6.21	0.91	4.30	1.32	5.41	1.05	2.75	2.06	2.05	2.76	4.31	1.31
R-50-5	4.67	2.20	2.12	3.27	1.43	2.54	1.84	3.38	1.38	1.83	2.55	0.51	9.13	2.50	1.87
Mean		1.96		1.37		2.16		1.50		2.38		7.23		1.72	
Standard deviation		0.09		0.11		0.56		0.11		0.11		9.09		0.08	
Coefficient of variation		0.15		0.25		0.34		0.22		0.14		0.42		0.16	
S-30-5	2.42	2.20	1.10	2.76	0.88	1.95	1.24	2.34	1.03	1.83	1.32	0.31	7.88	0.88	2.75
S-40-0	1.66	1.72	0.97	0.00	0.00	0.85	1.95	2.01	0.83	1.52	1.09	0.00	0.00	0.52	3.19
S-40-5	3.06	2.20	1.39	3.08	0.99	2.31	1.32	2.95	1.04	1.83	1.67	0.31	9.97	0.88	3.47
S-40-9	2.43	2.69	0.90	4.36	0.56	3.10	0.78	3.73	0.65	2.14	1.14	0.62	3.95	1.24	1.95
S-40-17	3.58	3.65	0.98	6.21	0.58	4.30	0.83	5.41	0.66	2.75	1.30	1.23	2.91	1.97	1.82
S-50-5	2.75	2.20	1.25	3.27	0.84	2.54	1.08	3.38	0.81	1.83	1.50	0.31	8.96	0.88	3.12
Mean		1.10		0.77		1.20		0.84		1.34		6.73		2.72	
Standard deviation		0.03		0.03		0.15		0.02		0.04		7.83		0.39	
Coefficient of variation		0.16		0.22		0.32		0.18		0.15		0.42		0.23	

Note: The mean, deviation and coefficient of variation are for the ratio of $v_r/V_{Eq.(i)}$



shear failure occurred, the slippages increased gradually with the decreasing of interface shear stress until reaching constant. This type of relationship between horizontal shear stress and interface slippage has been observed in beams with rough interface condition, except for Beam R-40-17 (flexural failure) and Beam R-40-9 (earlier shear failure of interface, see Fig. 10a). As mentioned previously, Beam R-40-17 did not fail in horizontal shear but in flexural causing the different horizontal shear stress-slip relation. As for Beam R-40-9, horizontal shear stress increased with the increasing of interface slippage at first. Then decreasing of horizontal shear stress occurred, with the observed interface shear crack progressing

nearly the entire length of beam. However, the interface did not fail in horizontal shear completely, causing the increasing of horizontal shear stress again. After shear failure of interface occurred (ultimate horizontal shear stress), the horizontal shear stress dropped to a constant value. This phenomenon indicated that composite beam also had capacity after interface shear failure occurred. Table 7 summarizes the failure horizontal shear stress, maximum horizontal shear stress, slippage at failure shear stress and slippage at maximum shear stress. To be compared, the horizontal shear stress corresponded to the slip of 0.13 mm (suggested as the slip limit of horizontal shear failure by Hanson (1960)) and the slip of

Table 7 Physical properties of test beams.

Specimens number	ρ_f (MPa)	Concrete strength f'_c (MPa)	Horizontal shear stress (MPa)				Slip (mm)		Failure mode
			At 0.13 mm slip	At 0.5 mm slip	At failure	Maximum	At failure	At maximum shear stress	
R-30-5	0.60	30.03	1.59	4.65	4.83	4.83	0.63	0.63	Horizontal shear
R-40-0	0.00	40.10	0.48	1.38	3.03	3.03	0.82	0.82	Horizontal shear
R-40-5	0.60	42.24	0.82	2.08	5.28	5.28	1.13	1.13	Horizontal shear
R-40-9	1.21	40.73	0.49	1.20	4.62	4.87	1.65	2.88	Horizontal shear
R-40-17	2.41	40.64	0.36	1.57	5.67	5.67	1.40	1.40	Flexure
R-50-5	0.60	50.71	0.39	0.86	4.67	4.67	1.38	1.38	Horizontal shear
S-30-5	0.60	30.03	0.71	1.50	2.42	3.21	1.48	6.38	Horizontal shear
S-40-0	0.00	40.10	0.75	1.49	1.66	2.44	0.62	5.38	Horizontal shear
S-40-5	0.60	42.24	0.28	1.31	3.06	3.20	1.01	5.91	Horizontal shear
S-40-9	1.21	40.73	1.10	2.25	2.43	3.33	1.17	5.37	Horizontal shear
S-40-17	2.41	40.64	0.67	2.21	3.58	4.41	1.53	5.04	Horizontal shear
S-50-5	0.60	50.71	0.44	1.48	2.75	3.01	0.81	4.66	Horizontal shear

0.50 mm (suggested as the slip limit of horizontal shear failure by Loov and Patnaik (1994)) are listed in Table 7. From the test results, it seemed that no clear relationship between interface shear slippage and interface shear failure existed.

From Table 7 and Fig. 10, it can also be found that the interface preparation method influenced the horizontal shear stress of composite beam effectively. This highlights the importance of aggregate interlock action for interface shear capacity. It can also be found that there is no obvious trend that can be established to describe the influence of concrete strength on the horizontal shear stress of composite beams, which was consistent with the results from Patnaik (2001). The higher horizontal shear capacity of composites beams with the target slab concrete strength of 40 MPa may be associated with its higher splitting tensile strength as shown in Table 3. With the increasing of clamping stress (from 0 to 0.60 MPa), there is no doubt that specimens with higher clamping stress got a higher value of interface shear stress. However, when the clamping stress increased from 0.60 to 1.21 MPa, interface shear stress decreased. A possible explanation for this unusual phenomenon may be the non-simultaneous shear failure of interface. As discussed in Part 4.2, this resulted in the shear capacity of interface reinforcements cannot reach yielding simultaneously and this unusual appearance had also been found in the recent research (Sneed et al. 2016; Jiang et al. 2016). These indicate the necessity for retaining an upper limit for horizontal shear stress. Higher clamping stress would not certainly promote the interface shear capacity. Without reaching interface shear failure, Beam R-40-17 and Beam S-40-17 reached a higher horizontal shear capacity.

On the other hand, higher slab concrete strength and higher clamping stress caused a larger slip at horizontal shear failure.

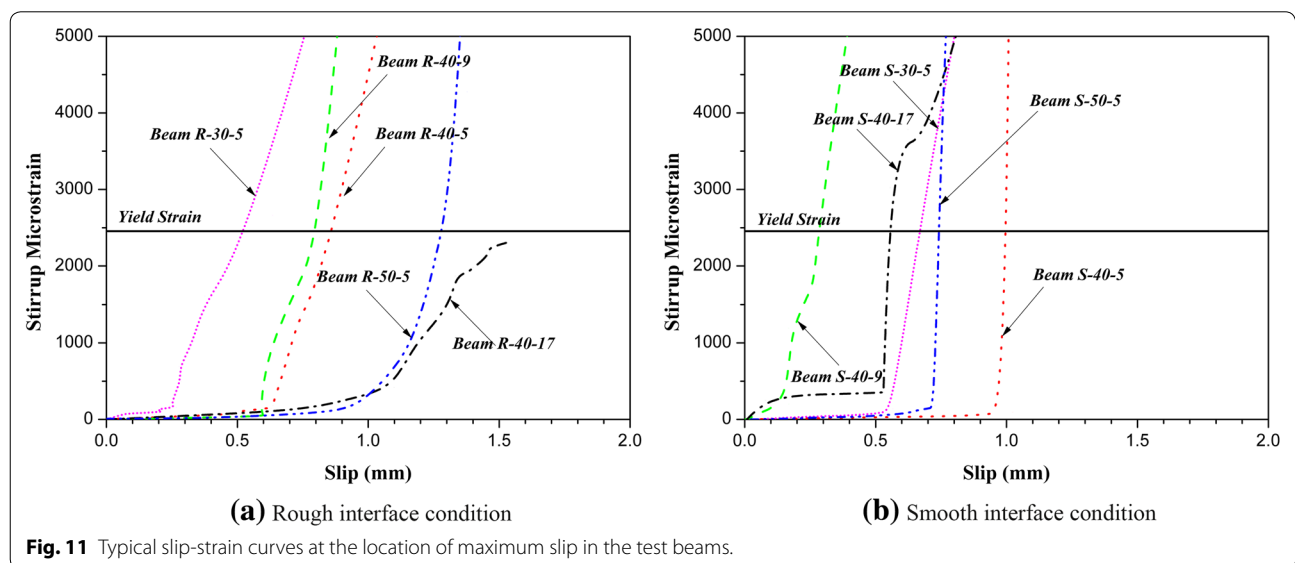
4.5 Stirrup Stresses

As shown in Fig. 1c, several strain gauges were glued on selected stirrups at the location of interface. The stirrups near the center-span were not effective and they became increasingly effective with increasing distance from the center up to the end of flange. Coincidentally, the maximum interface slip and maximum stirrup strain always occurred at the same location. The strain of shear reinforcement crossing the interface is plotted versus interface slip at this location in Fig. 11, maintaining the distinction between beams with different slab concrete strength and different clamping stress. The stirrup strains increased with the increasing of slip. The stirrup stresses were much lower than yielding strength until a slip of 0.5 mm or higher occurred for beams failed in horizontal shear. Before horizontal shear failure occurred, most stirrups reached the yielding strength at a slip between 0.5 and 1.0 mm. However, it seemed that no clear relationship between interface shear slippage and interface shear failure existed.

5 Recommendation

5.1 Proposed Shear Capacity Equation and Verification

As shown in Table 6, the capacity of specimens presented in this study can rarely be predicted well by existing equations. Thus, a more applicable model is necessary for predicting the shear strength of interface between normal weight and lightweight concrete. Similar to the proposals of several authors, multiple regression analysis was



performed to propose an equation adjusted to the results presented in this study. In order to consider the influence of clamping stress and lightweight concrete strength, the regression analysis was based on Kahn and Mitchell's equation. The proposed horizontal shear capacity equation is composed as described in Eq. (9), incorporating a component for bond and interlock action ($\alpha f'_c$) and a friction component of clamping stress (βf_y):

$$v_n = \alpha f'_c + \beta \rho f_y \quad (9)$$

where, α and β are values acquired by the regression analysis on the experimental results. Therefore, the value of $\alpha = 0.10$ and $\beta = 0.85$ for rough interface condition, and $\alpha = 0.05$ and $\beta = 0.6$ for smooth interface condition can be obtained.

For rough interface condition:

$$v_n = 0.10 f'_c + 0.85 \rho f_y \quad (10)$$

But not more than $K_1 f'_c$ nor K_2

For smooth interface condition:

$$v_n = 0.05 f'_c + 0.6 \rho f_y \quad (11)$$

But not more than $K_3 f'_c$ nor K_4

Similar to that used by AASHTO 2015, ACI 318-14 or other researchers (e.g., Mattock et al. 1976; Loov and Patnaik 1994; Kahn and Mitchell 2002; Harries et al. 2012), an upper limit for the interface shear strength was set to agree well with the experimental data. For lightweight concrete with rough interface condition, $K_1 = 0.3$; and $K_2 = 9$ MPa; for normal weight concrete with rough interface condition, $K_1 = 0.3$; and $K_2 = 12$ MPa; while for the case of high-strength concrete with rough interface condition, $K_1 = 0.3$; and $K_2 = 15$ MPa. For smooth interface condition, $K_3 = 0.2$; and $K_4 = 9$ MPa for lightweight concrete, normal weight concrete and high-strength concrete. For both smooth and rough interface condition, the predicted results show a good agreement with those obtained from experimental and analytical values. The mean value and standard deviation between experimental and predicted value by Eq. (10) are 1.00 and 0.22 for rough interface condition, respectively. While for smooth interface condition, the relation and standard deviation between experimental and predicted value by Eq. (11) are 1.03 and 0.18, respectively.

5.2 Validation of the Proposed Equation

In order to assess the applicability of Eqs. (10) and (11), the related experimental results obtained by Saemann and Washa (1964), Mattock (1976), Mattock et al. (1976), Hoff (1992), Loov and Patnaik (1994), Patnaik (2001), Kahn and Mitchell (2002), Kahn and Slapkus (2004), Mansur et al. (2008), Shaw and Sneed (2014), and Sneed et al. (2016) were considered. The source and specimens

results are listed in Tables 8 and 9, including results of normal weight concrete composite beam test (NWB), lightweight concrete push-off test (LCP), normal weight concrete push-off test (NWP), and high-strength concrete push-off test (HSP). Additionally, all of these specimens were failed in interface shear. Table 10 shows the comparison of proposed equation with the experimental results of other researchers listed above. To be clear, the evaluation of proposed interface shear resistance equation is also plotted in Fig. 12. It can be seen that Eq. (10) gave a conservative predicted for HSP with value of 0.79 for the mean of predicted/experimental results. On the contrary, Eq. (10) represented an accurate prediction for NWB, LCP and NWP with rough shear plane. For smooth interface condition, the average mean values of predicted to experimental results is 1.11, which demonstrates that the Eq. (11) can be potentially used to predict the smooth interface shear capacity of composite beam test, or the push-off test made of normal weight, lightweight or high-strength concrete. However, the authors suggest that more experimental data of interface shear resistance between normal weight and lightweight concrete are needed to verify the applicability of the proposed empirical equations and interlock action.

6 Conclusions

Bridges constructed with precast normal weight concrete girder and lightweight concrete slab have been widely used in many bridge projects. Based on the results of this research, the main conclusions are drawn as follows.

- (1) Most composite beam failed in horizontal shear exhibiting clearly visible separation of flange and web and horizontal crack along the horizontal shear interface. Several flexure cracks appeared in the bottom of flange while lots of crush crack formed at the top of web after interface shear failure. More flexural cracks or vertical shear cracks were observed at specimens with rough interface condition, with higher interface shear reinforcement ratios or with lower lightweight concrete strength.
- (2) Both interface shear capacity and vertical deflection at horizontal shear failure load appeared to be influenced by interface preparation method and clamping stress, but insensitive to the compressive strength of lightweight slab concrete.
- (3) Interfaces prepared method, clamping stress and lightweight slab concrete strength played an important role in interface slippage at horizontal shear failure.
- (4) Most stirrups reached the yielding strength at a slip between 0.5 and 1.0 mm before horizontal shear failure occurred, and it seemed that no clear rela-

Table 8 Experimental results of other researchers' with rough interface condition.

Concrete type	Author	Specimens	f'_c (MPa)	ρ	f_y (MPa)	ρf_y (MPa)	v (MPa)		
NWB	Saemann and Washa (1964)	8A	20.13	0.0108	293.73	3.18	4.26		
		6A	20.00	0.0102	293.73	3.00	6.57		
	Loov and Patnaik (1994)	Beam 1	37.40	0.0100	438.00	4.36	7.76		
		Beam 2	34.90	0.0038	438.00	1.66	4.27		
		Beam 3	30.50	0.0064	432.00	2.76	6.82		
		Beam 5	34.80	0.0038	430.00	1.63	5.54		
		Beam 6	37.10	0.0038	428.00	1.62	5.25		
		beam 7	35.80	0.0140	432.00	6.06	9.25		
		Beam 8	35.60	0.0019	407.00	0.77	3.12		
		Beam 9	37.10	0.0038	428.00	1.62	4.64		
		Beam 10	37.60	0.0019	409.00	0.77	3.46		
		Beam 12	34.60	0.0189	408.00	7.72	9.20		
		Beam 13	19.20	0.0019	431.00	0.82	2.92		
		Kahn and Slapkus (2004)	7-5	50.20	0.0019	556.00	1.03	4.09	
			7-7	50.20	0.0028	556.00	1.55	6.77	
7-9	50.20		0.0037	556.00	2.06	6.90			
LCP	Mattock et al. (1976)	A0	29.17	0.0000	0.00	0.00	3.45		
		A1	25.79	0.0044	328.89	1.45	5.23		
		A2	28.24	0.0088	369.57	3.25	6.30		
		A3	26.96	0.0132	366.81	4.84	7.03		
		A4	28.27	0.0176	350.96	6.18	7.58		
		A5	27.30	0.0220	350.96	7.72	8.21		
		A6	29.30	0.0264	357.16	9.43	9.27		
	Shaw and Sneed (2014)	S-5-R-1	31.37	0.0133	456.00	6.06	7.17		
		S-5-R-2	31.37	0.0133	456.00	6.06	7.03		
		S-5-R-3	31.37	0.0133	456.00	6.06	7.52		
		S-8-R-1	49.71	0.0133	456.00	6.06	10.07		
		S-8-R-2	49.71	0.0133	456.00	6.06	9.38		
		S-8-R-3	49.71	0.0133	456.00	6.06	9.31		
	Sneed et al. (2016)	S-SL-CJ-R-9-1	37.10	0.0090	498.00	4.48	6.90		
		S-SL-CJ-R-9-2	37.10	0.0090	498.00	4.48	7.03		
		S-SL-CJ-R-13-1	38.41	0.0130	498.00	6.47	8.80		
		S-SL-CJ-R-13-2	38.41	0.0130	498.00	6.47	8.27		
		S-SL-CJ-R-17-1	34.13	0.0170	498.00	8.47	8.69		
		S-SL-CJ-R-17-2	34.13	0.0170	498.00	8.47	9.10		
		S-SL-CJ-R-22-1	34.48	0.0220	498.00	10.96	8.96		
		S-SL-CJ-R-22-2	34.48	0.0220	498.00	10.96	8.00		
		S-CL-CJ-R-9-1	32.89	0.009	498.00	4.48	5.17		
		S-CL-CJ-R-9-2	32.89	0.0090	498.00	4.48	6.76		
		S-CL-CJ-R-13-1	31.99	0.0130	498.00	6.47	7.07		
		S-CL-CJ-R-13-2	31.99	0.0130	498.00	6.47	6.53		
		NWP	Mattock et al. (1976)	M0	27.13	0.0000	0.00	0.00	4.07
				M1	28.82	0.0044	350.96	1.54	5.24
M2	26.89			0.0088	363.37	3.20	6.76		
M3	27.55			0.0132	360.61	4.76	7.65		
M4	28.61			0.0176	350.96	6.18	7.86		
M5	27.13			0.0220	363.37	8.00	8.48		
M6	28.41			0.0264	363.37	9.60	9.10		

Table 8 (continued)

Concrete type	Author	Specimens	f'_c (MPa)	ρ	f_y (MPa)	ρf_y (MPa)	v (MPa)
	Mattock (1976)	B1	40.27	0.0044	353.51	1.56	3.36
		B2	40.27	0.0088	348.54	3.07	4.83
		B3	41.75	0.0132	353.51	4.66	7.27
		B4	41.75	0.0176	371.09	6.53	8.80
		B5	40.65	0.0256	339.58	8.70	10.83
		B6	40.65	0.0320	339.58	10.87	11.72
		D1	25.99	0.0044	353.51	1.55	4.07
		D2	25.99	0.0088	353.51	3.11	6.34
		D3	20.27	0.0132	386.12	5.10	6.96
		D4A D4	17.20 20.27	0.0176 0.0176	372.33 386.12	6.55 6.79	6.85 6.91
	Mansur et al. (2008)	AN-2	40.20	0.0089	530.00	4.71	8.18
		AN-4	40.20	0.0178	530.00	9.42	10.17
		AN-6	40.20	0.0267	530.00	14.13	12.92
	Shaw and Sneed (2014)	N-5-R-4	33.51	0.0133	456.00	6.06	8.21
		N-5-R-5	33.51	0.0133	456.00	6.06	7.45
		N-5-R-6	33.51	0.0133	456.00	6.06	7.45
		N-8-R-1	52.06	0.0133	456.00	6.06	10.34
		N-8-R-2	52.06	0.0133	456.00	6.06	7.79
		N-8-R-3	52.06	0.0133	456.00	6.06	8.96
HSP	Kahn and Mitchell (2002)	SF-7-1-CJ	80.91	0.0051	413.70	2.10	6.21
		SF-7-2-CJ	80.91	0.0102	413.70	4.20	9.43
		SF-7-3-CJ	85.99	0.0152	413.70	6.30	12.67
		SF-7-4-CJ	85.99	0.0203	413.70	8.39	15.24
		SF-10-3-CJ	89.31	0.0152	413.70	6.30	13.09
		SF-10-4-CJ	89.31	0.0203	413.70	8.39	14.49
		SF-14-1-CJ	101.74	0.0051	413.70	2.10	10.45
		SF-14-2-CJ	101.74	0.0102	413.70	4.20	11.40
		SF-14-3-CJ	104.93	0.0152	413.70	6.30	15.48
		SF-14-4-CJ	104.93	0.0203	413.70	8.39	17.60
	Mansur et al. (2008)	AM-2	69.00	0.0089	530.00	4.71	7.50
		AM-3	69.00	0.0133	530.00	7.07	11.50
		AM-4	69.00	0.0178	530.00	9.42	14.03
		AH-2	87.00	0.0089	530.00	4.71	7.78
		AH-3	87.00	0.0133	530.00	7.07	12.36
		AH-4	87.00	0.0178	530.00	9.42	14.17
		B1-4	73.20	0.0089	300.00	2.67	6.73
		B2-2	84.90	0.0042	300.00	1.34	5.17
		B2-4	84.90	0.0089	300.00	2.67	7.32
		B2-5	84.90	0.0112	300.00	3.36	8.21
		B2-6	84.90	0.0134	300.00	4.02	9.17
		B3-4	95.20	0.0089	300.00	2.67	7.97
		B4-2	106.40	0.0045	300.00	1.34	6.01
		B4-4	106.40	0.0089	300.00	2.67	8.43
	B4-5	106.40	0.0112	300.00	3.36	9.24	
	B4-6	106.40	0.0134	300.00	4.02	9.96	

Note: *NWB* = normal weight concrete composite beam test specimens; *LCP* = lightweight concrete push-off test specimens; *NWP* = normal weight concrete push-off test specimens; *HSP* = high-strength concrete push-off test specimens.

Table 9 Experimental results of other researchers' with smooth interface condition.

Concrete type	Author	Specimens	f'_c (MPa)	ρ	f_y (MPa)	ρf_y (MPa)	v (MPa)	
NWB	Loov and Patnaik (1994)	Beam 14	19.60	0.0019	431.00	0.82	1.93	
		Patnaik (2001)	SR1.1	19.80	0.0005	558.00	0.30	1.78
			SR1.2	19.80	0.0005	558.00	0.30	2.37
			SR2.1	23.50	0.0014	520.00	0.75	1.89
			SR2.2	23.50	0.0014	520.00	0.75	1.61
			SR3.1	17.00	0.0008	704.00	0.59	1.91
			SR3.2	17.00	0.0008	704.00	0.59	1.73
			SR4.1	34.80	0.0007	641.00	0.44	1.74
			SR4.2	26.70	0.0007	641.00	0.44	1.35
			SR4.3	34.80	0.0012	641.00	0.79	1.48
			SR4.4	26.70	0.0012	641.00	0.79	1.53
			SR4.5	34.80	0.0018	641.00	1.14	2.99
			SR4.6	26.70	0.0018	641.00	1.14	1.94
			SR5.1	34.80	0.0025	641.00	1.59	2.11
			SR5.2	26.70	0.0025	641.00	1.59	2.25
			SR5.3	34.80	0.0031	641.00	1.99	3.01
			SR5.4	26.70	0.0031	641.00	1.99	2.81
			SR5.5	34.80	0.0041	641.00	2.65	4.56
			SR5.6	26.70	0.0041	641.00	2.65	4.13
			ST1.1	34.40	0.0052	340.00	1.78	3.16
		ST1.2	32.40	0.0052	340.00	1.78	3.61	
		ST2.1	33.90	0.0070	340.00	2.37	4.70	
		ST2.2	31.60	0.0070	340.00	2.37	5.08	
		ST3.1	26.90	0.0105	340.00	3.56	5.90	
		ST3.2	30.30	0.0105	340.00	3.56	6.30	
LCP	Mattock et al. (1976)	B1	25.79	0.0044	341.99	1.50	3.10	
		B2	23.17	0.0088	350.96	3.09	4.50	
		B3	26.96	0.0132	350.96	4.63	5.79	
		B4	28.27	0.0176	338.54	5.96	6.48	
		B5	27.30	0.0220	348.20	7.66	6.90	
		B6	29.30	0.0264	357.16	9.43	7.96	
		D1	41.34	0.0044	357.16	1.57	2.55	
		D2	41.34	0.0088	360.61	3.17	4.61	
		D3	39.37	0.0132	360.61	4.76	5.32	
		D4	39.37	0.0176	360.61	6.34	7.05	
			D5	38.61	0.0220	360.61	7.94	7.46
			D6	38.61	0.0264	357.16	9.43	8.41
	Hoff (1992)	LWC1-1	58.54	0.0052	370.00	1.94	1.98	
		LWC1-2	58.68	0.0052	370.00	1.94	2.52	
		LWC1-3	57.16	0.0052	370.00	1.94	2.85	
		LWC1-4	58.54	0.0095	469.00	4.47	5.25	
		LWC1-5	58.68	0.0095	476.00	4.53	4.69	
		LWC1-6	57.16	0.0095	469.00	4.47	5.01	
		LWC2-1	63.92	0.0052	370.00	1.93	3.37	
		LWC2-2	60.40	0.0052	370.00	1.93	2.31	
LWC2-3		60.19	0.0052	370.00	1.93	2.06		
LWC2-4		57.02	0.0095	469.00	4.47	5.10		
		LWC2-5	60.40	0.0095	472.00	4.50	4.77	
		LWC2-6	60.19	0.0095	472.00	4.50	4.69	

Table 9 (continued)

Concrete type	Author	Specimens	f'_c (MPa)	ρ	f_y (MPa)	ρf_y (MPa)	v (MPa)
		LWC3-1	71.09	0.0053	497.00	2.61	4.61
		LWC3-2	75.22	0.0053	497.00	2.61	3.78
		LWC3-3	75.98	0.0053	497.00	2.61	4.03
		LWC3-4	71.09	0.0095	461.00	4.36	6.00
		LWC3-5	75.22	0.0096	461.00	4.41	6.00
		LWC3-6	75.98	0.0095	461.00	4.39	6.16
	Shaw and Sneed (2014)	S-5-S-1	31.37	0.0133	456.00	6.06	5.38
		S-5-S-2	31.37	0.0133	456.00	6.06	4.76
		S-5-S-3	31.37	0.0133	456.00	6.06	5.52
		S-8-S-1	49.71	0.0133	456.00	6.06	9.31
		S-8-S-2	49.71	0.0133	456.00	6.06	8.07
		S-8-S-3	49.71	0.0133	456.00	6.06	8.21
	Sneed et al. (2016)	S-SL-CJ-S-9-1	37.10	0.009	498.00	4.48	3.72
		S-SL-CJ-S-9-2	37.10	0.009	498.00	4.48	4.55
		S-SL-CJ-S-13-1	38.41	0.013	498.00	6.47	5.50
		S-SL-CJ-S-13-2	38.41	0.013	498.00	6.47	6.79
		S-SL-CJ-S-17-1	34.13	0.017	498.00	8.47	6.62
		S-SL-CJ-S-17-2	34.13	0.017	498.00	8.47	6.55
		S-SL-CJ-S-22-1	34.48	0.022	498.00	10.96	6.96
		S-SL-CJ-S-22-2	34.48	0.022	498.00	10.96	7.86
		S-CL-CJ-S-9-1	32.89	0.009	498.00	4.48	4.48
		S-CL-CJ-S-9-2	32.89	0.009	498.00	4.48	5.31
		S-CL-CJ-S-13-1	31.99	0.013	498.00	6.47	5.71
		S-CL-CJ-S-13-2	31.99	0.013	498.00	6.47	5.63
		S-CL-CJ-S-17-1	31.37	0.017	498.00	8.47	6.00
		S-CL-CJ-S-17-2	31.37	0.017	498.00	8.47	6.83
NWP	Mattock et al. (1976)	N1	28.82	0.0044	350.96	1.54	3.17
		N2	26.89	0.0088	363.37	3.20	5.38
		N3	27.55	0.0132	360.61	4.76	6.62
		N4	28.61	0.0176	350.96	6.18	7.93
		N5	27.13	0.0220	350.96	7.72	8.10
		N6	28.41	0.0264	344.75	9.10	8.21
	Kahn and Mitchell (2002)	SF-4-1-C	46.92	0.00425	413.70	1.76	4.02
		SF-4-2-C	46.92	0.00850	413.70	3.52	6.40
		SF-4-3-C	46.92	0.01275	413.70	5.27	8.18
	Shaw and Sneed (2014)	N-5-S-4	33.51	0.0133	456.00	6.06	4.55
		N-5-S-5	33.51	0.0133	456.00	6.06	4.83
		N-5-S-6	33.51	0.0133	456.00	6.06	5.45
		N-8-S-1	52.06	0.0133	456.00	6.06	9.10
		N-8-S-2	52.06	0.0133	456.00	6.06	7.45
		N-8-S-3	52.06	0.0133	456.00	6.06	7.72
HSP	Kahn and Mitchell (2002)	SF-10-1-CJ	98.78	0.00507	413.70	2.10	3.65
		SF-10-2-CJ	83.11	0.01015	413.70	4.20	5.67

Note: *NWB* = normal weight concrete composite beam test specimens; *LCP* = lightweight concrete push-off test specimens; *NWP* = normal weight concrete push-off test specimens; *HSP* = high-strength concrete push-off test specimens.

Table 10 Comparison of proposed equation with other researchers' experimental results.

Interface condition	Concrete type	Author	Mean		Standard deviation			Coefficient of variation			
Rough interface	NWB	Saemann and Washa (1964)	0.99	1.00	0.94	0.15	0.19	0.19	0.15	0.19	0.20
		Loov and Patnaik (1994)	0.93		0.17			0.18			
		Kahn and Slapkus (2004)	1.17		0.27			0.23			
	LCP	Mattock et al. (1976)	1.10	0.98	0.13	0.13	0.12	0.14			
		Shaw and Sneed (2014)	0.97		0.10			0.10			
		Sneed et al. (2016)	0.90		0.09			0.10			
	NWP	Mattock et al. (1976)	1.17	1.00	0.16	0.18	0.14	0.18			
		Mattock (1976)	0.89		0.08			0.09			
		Mansur et al. (2008)	0.95		0.16			0.17			
	HSP	Kahn and Mitchell (2002)	0.91	0.79	0.14	0.16	0.15	0.20			
Mansur et al. (2008)		0.72		0.12			0.17				
Smooth interface	NWB	Loov and Patnaik (1994)	1.31	1.25	1.11	0.00	0.34	0.30	0.00	0.27	0.27
		Patnaik (2001)	1.25		0.35			0.28			
	LCP	Mattock et al. (1976)	1.20	1.00	0.21	0.24	0.18	0.23			
		Hoff (1992)	1.03		0.10			0.10			
		Shaw and Sneed (2014)	1.20		0.17			0.14			
	NWP	Sneed et al. (2016)	0.78		0.16			0.20			
		Mattock et al. (1976)	1.51	1.32	0.10	0.24	0.06	0.18			
		Kahn and Mitchell (2002)	1.11		0.21			0.19			
	HSP	Shaw and Sneed (2014)	1.37		0.13			0.10			
		Kahn and Mitchell (2002)	0.72	0.70	0.13	0.13	0.18	0.19			

Note: *NWB* = normal weight concrete composite beam test specimens; *NWP* = normal weight concrete push-off test specimens; *LCP* = lightweight concrete push-off test specimens; *HSP* = high-strength concrete push-off test specimens.

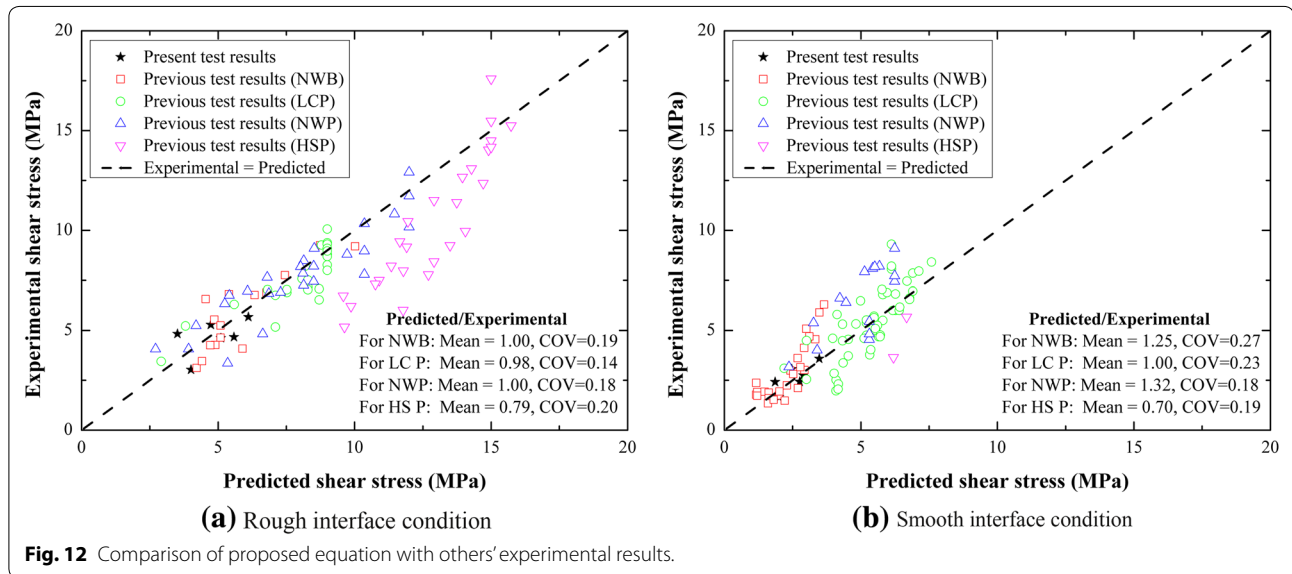


Fig. 12 Comparison of proposed equation with others' experimental results.

relationship between interface shear slippage and interface shear failure existed.

- (5) Eq. (1) and Eq. (3) predicted the horizontal shear stress of smooth interface well but underestimated

that of rough interface condition. On the contrary, Eq. (2) and Eq. (4) gave an acceptable prediction for rough interface shear behavior but overestimated that of smooth interface condition. The other three

types of current design provisions predicted the interface shear capacity conservatively.

- (6) A more accurate equation has been proposed to give an more accurate predict for interface shear capacity of normal weight concrete and lightweight concrete composite T-beam. Compared with previous research, this proposed formula represented the best results, which is reasonably well, for different types of concrete with both rough interface condition and smooth interface condition.

Authors' contributions

ZF designed and performed the experiments, as well as drafted the manuscript. HJ have carried the literature study and participated in discussing the results. AL provided some advices on the manuscript. JF and YC performed the experimental works. All authors read and approved the final manuscript.

Author details

¹ School of Civil and Transportation Engineering, Guangzhou Higher Education Mega Center, Guangdong University of Technology, Guangzhou 510006, China. ² Guangzhou University-Tamkang University Joint Research, Center for Engineering Structure Disaster Prevention and Control, Guangzhou Higher Education Mega Center, Guangzhou University, Guangzhou 510006, China.

Acknowledgements

The research presented was funded by National Natural Science Foundation of China (51778150), Science and Technology Planning Project of Guangdong Province (2016B050501004) and Science and Technology Planning Project of Guangzhou City (201.804.010.422). The authors gratefully acknowledge their generous support and declare that they have no conflict of interest.

Publisher's Note

Springer Nature remains neutral with regard to jurisdictional claims in published maps and institutional affiliations.

Received: 7 September 2017 Accepted: 16 April 2018

Published online: 02 August 2018

References

- ACI Committee 318. (2014). *Building code requirements for structural concrete (ACI 318-14)*. Farmington Hills: American Concrete Institute (ACI).
- American Association of State Highway and Transportation Officials (AASHTO). (2015). *AASHTO bridge design specifications* (7th ed.). Washington, DC: AASHTO.
- American Society for Testing and Materials (ASTM). (2011). *Standard test method for splitting tensile strength of cylindrical concrete specimens. (ASTM C496/C496 M-11)*. West Conshohocken, PA, US: ASTM.
- American Society for Testing and Materials (ASTM). (2014). *Standard test method for static modulus of elasticity and Poisson's ratio of concrete in compression. (ASTM C469/C469 M-14)*. West Conshohocken: ASTM.
- American Society for Testing and Materials (ASTM). (2015). *Standard practice for use of unbond caps in determination of compressive strength of hardened*

- cylindrical concrete specimens. (ASTM C1231/C1231 M-15)*. West Conshohocken: ASTM.
- American Society for Testing and Materials (ASTM). (2017). *Standard test method for density (Unit Weight), yield, and air content (gravimetric) of concrete (ASTM C138/C138M-17a)*. West Conshohocken: ASTM.
- Bass, R. A., Carrasquillo, R. L., & Jirsa, J. O. (1989). Shear transfer across new and existing concrete interfaces. *ACI Structural Journal*, 86(4), 383–393.
- Birkeland, P. W., & Birkeland, H. W. (1966). Connections in precast concrete construction. *ACI Structural Journal*, 63(3), 345–368.
- Hanson, N. W. (1960). Precast-Prestressed concrete bridges 2. Horizontal shear connections. *Journal of the PCA Research and Development Laboratories*, 2(2), 38–60.
- Harries, K. A., Zeno, G., & Shahrooz, B. (2012). Toward an improved understanding of shear-friction behavior. *ACI Structural Journal*, 109(6), 835–844.
- Hoff, G. C. (1992). High-strength lightweight aggregate concrete for arctic applications-Part 3. In T. A. Holm & A. M. Vaysburd (Eds.), *Structural Lightweight Aggregate Concrete Performance, SP-136* (pp. 175–245). Farmington Hills: American Concrete Institute.
- Jiang, H. B., Fang, Z. C., Liu, A. R., Li, Y. H., & Feng, J. H. (2016). Interface shear behavior between high-strength precast girders and lightweight cast-in-place slabs. *Construction and Building Materials*, 128, 449–460.
- Kahn, L. F., & Mitchell, A. D. (2002). Shear-friction tests with high-strength concrete. *ACI Structural Journal*, 99(1), 98–103.
- Kahn, L. F., & Slapkus, A. (2004). Interface shear in high strength composite T-beams. *PCI Journal*, 49(4), 102–110.
- Loov, R. E., & Patnaik, A. K. (1994). Horizontal shear strength of composite concrete beams with a rough interface. *PCI Journal*, 39(1), 48–69.
- Mansur, M. A., Vinayagam, T., & Tan, K. H. (2008). Shear transfer across a crack in reinforced high-strength concrete. *Journal of Materials in Civil Engineering*, 20(4), 294–302.
- Mattock, A. H. (1974). Shear transfer in concrete having reinforcement at an angle to the shear plane. *ACI Structural Journal*, 42(2), 17–42.
- Mattock, A. H. (1976). *Shear transfer under monotonic loading across an interface between concrete cast at different times Report SM 76-3*. Seattle: University of Washington Department of Civil Engineering.
- Mattock, A. H., & Hawkins, N. M. (1972). Shear transfer in reinforced concrete—recent research. *PCI Journal*, 17(2), 55–75.
- Mattock, A. H., Li, W. K., & Wang, T. C. (1976). Shear transfer in lightweight reinforced concrete. *PCI Journal*, 21(1), 20–39.
- Patnaik, A. K. (2001). Behavior of composite concrete beams with smooth interface. *Journal of Structural Engineering*, 127(4), 359–366.
- Saemann, J. C., & Washa, G. W. (1964). Horizontal shear connections between precast beams and cast-in-place slabs. *Journal American Concrete Institute*, 61(11), 1383–1408.
- Shaw, D. M., & Sneed, L. H. (2014). Interface shear transfer of lightweight-aggregate concretes cast at different times. *PCI Journal*, 59(3), 130–144.
- Sneed, L. H., Krc, K., Wermager, S., & Meinheit, D. (2016). Interface shear transfer of lightweight-aggregate concretes with different lightweight aggregates. *PCI Journal*, 61(2), 38–55.
- Walraven, J. (1987). Influence of concrete strength and load history on the shear-friction capacity of concrete members. *PCI Journal*, 32(1), 66–84.

Submit your manuscript to a SpringerOpen® journal and benefit from:

- Convenient online submission
- Rigorous peer review
- Open access: articles freely available online
- High visibility within the field
- Retaining the copyright to your article

Submit your next manuscript at ► springeropen.com